



## PLASTICITY-DAMAGE MATERIAL CONSTITUTIVE MODEL FOR TIMBER SUBJECTED TO CYCLIC LOADING

L.F. Sirumbal-Zapata<sup>(1)</sup>, C. Málaga-Chuquitaype<sup>(2)</sup>, A.Y. Elghazouli<sup>(3)</sup>

<sup>(1)</sup> PhD student, Department of Civil and Environmental Engineering, Imperial College London, l.sirumbal-zapata14@imperial.ac.uk

<sup>(2)</sup> Lecturer, Department of Civil and Environmental Engineering, Imperial College London, c.malaga@imperial.ac.uk

<sup>(3)</sup> Professor, Department of Civil and Environmental Engineering, Imperial College London, a.elghazouli@imperial.ac.uk

### **Abstract**

A plasticity-damage constitutive model for timber, which builds upon previous models developed for other quasi-brittle materials like concrete, is proposed in this article. Timber failure modes can be broadly defined as ductile failure due to compression stresses and brittle failure due to the combination of shear and tension stresses. This paper presents the formulation and implementation of a detailed and practical material constitutive model for timber subjected to cyclic loading, which can deal with both types of failure modes. Due to the anisotropic characteristics of timber, Hill's expression was used as equivalent stress damage criterion for both compressive and shear-tensile failure. The damage evolution process starts once the failure criterion is reached, and is handled by two different monotonically increasing functions of the equivalent stresses for tension (exponential softening) and compression (perfect plasticity). The damage variables associated with these functions gradually reduce the timber stiffness material parameters (elastic moduli and shear moduli). The main advantage of incorporating a continuous damage model for timber is to capture the post-elastic stiffness degradation and thus enable an accurate prediction of experimental results. On the other hand, plasticity allows the incorporation of timber plastic flow in compression and its associated permanent deformations. This study discusses the theoretical framework and consistency of both models and presents the equations required for their coupling and implementation. Preliminary numerical results are presented for uniaxial cyclic loading in both directions, parallel and perpendicular to the grain. It is shown that tensile softening brittle failure, stiffness cyclic degradation and recovery after load-reversal, in addition to compressive permanent plastic deformation, are key characteristics of the non-linear behaviour of timber. These characteristics can be captured by the proposed constitutive model, which represents the first step towards a faithful estimation of the earthquake-induced collapse capacity of timber structures.

*Keywords: timber; plasticity; damage; cyclic loading;*

## 1. Introduction

The structural performance of timber structures subjected to earthquake loading is governed by the nonlinear response in the connection zones, where high stress concentrations and large deformation levels are developed around the fasteners (nails, dowels or bolts). For this reason, the performance-based assessment of earthquake-resistant timber structures requires the implementation of a material constitutive model, which allows a faithful simulation of the nonlinear behaviour of these type of connections including large deformation levels until failure.

Timber failure modes can broadly be defined as ductile failure due to compression stresses and brittle failure due to the combination of shear and tension stresses. Therefore, in addition to the anisotropy of timber, the numerical modelling of this material involves the challenge of reproducing completely different failure modes and nonlinear responses for tensile and compressive stress regimes. Based on previous developments available for other quasi-brittle materials like concrete [1-3], this paper proposes a consistent and comprehensive 3D plasticity-damage material constitutive model for timber which is able to simulate the most important wood failure modes.

The plasticity component of the model simulates the ductile nonlinear behaviour and permanent deformation of timber under compressive stresses. On the other hand, the modelling of brittle shear and tensile failure is based on Continuum Damage Mechanics theory (CDM) which, although not suitable for explicit crack modelling, allows the monitoring of damage evolution and the identification of potential rupture zones through a smeared continuous approach. The coupling of plasticity and damage models is particularly attractive for materials with an inelastic behaviour characterized by the simultaneous occurrence of plastic flow and crack formation. Moreover, plasticity-damage models are able to reproduce the material stiffness degradation characteristic of cyclic loading problems subjected to extensive stress redistribution more accurately [4]. Nevertheless, in order to obtain reliable results, the thermodynamic consistency of the model should be verified to ensure that energy is dissipated and to avoid the introduction of spurious energy into the system [3].

In recent years, a few attempts have been made to develop a material constitutive model for timber subjected to monotonic loading that can deal with both ductile and brittle failure modes. However, to the authors' knowledge, no research has been done on timber constitutive models tailored to reproduce the cyclic response of wood. Most of the available timber models for monotonic loading employ plasticity theory for failure in compression. By contrast, two different approaches have been followed for shear and tension related failure modes. The first approach [5] is based on the nonlinear fracture theory for the definition of cohesive zone models, capable of simulating explicitly the crack formation and growth. The major disadvantages of this method are the complexity of the formulation and the practical difficulties associated with the determination of appropriate values for the input parameters. Furthermore, its implementation is generally feasible only for discrete crack modelling, which requires an a priori definition of the cracking path and severely limits its applicability to simulate timber dowelled connections subject to cyclic loading. The second approach, and the one followed herein, is based on CDM theory [6-8] and represents the best option for the definition of the plasticity-damage models of the form presented herein.

Among the various existing plasticity models for anisotropic materials, Hill and Hoffman have been frequently employed for modelling timber failure under monotonic loading exclusively. For example, Hill criterion was employed to develop a 2D elasto-plastic orthotropic model with anisotropic hardening [9], capable of simulating the biaxial (perpendicular and parallel to the grain) behaviour of timber under compression stresses only. Later, another model for timber was developed based on anisotropic plasticity with hardening for compression, and a simplified continuous damage model for shear and tension [7]. This plasticity-damage model was used to study the behaviour of timber-steel dowelled joints subjected to monotonic tension loads. Previously, the same model was employed in the study of the embedding strength of Glulam dowelled connections [10]. A different type of model for wood based on continuous damage mechanics exclusively was implemented, and its accuracy was evaluated based on experimental results of timber specimens subjected to monotonic tension, compression and dowel embedment tests [6]. More recently, a model within the framework of plasticity coupled with continuous damage mechanics, was developed for the study of brittle failure modes of

dowelled timber-steel connections subjected to monotonic tension loading [8]. This refined constitutive model incorporates the effects of orthotropic elasticity, anisotropic plasticity with isotropic hardening, isotropic ductile damage, and large plastic deformations. Nonetheless, the model does not consider different input strength parameters for tension and compression failure.

This paper describes the implementation of a 3D material constitutive model for wood that is capable to reproduce its cyclic response and failure modes, through the coupling of an orthotropic Hill plasticity model with isotropic hardening, and an isotropic continuous damage model. To this end, the next section discusses the nonlinear experimental response and failure characteristics of wood under compression, tension and shear stresses. This is followed by a presentation of the theoretical basis and constitutive equations of the elasticity and damage parts of the proposed model in Sections 3 and 4, respectively. The plasticity formulation is developed in Section 5. Section 6 shows the application of the proposed model in simulating the uniaxial cyclic response of timber in the directions parallel and perpendicular to the grain. Finally, general conclusions are offered in Section 7.

## 2. Nonlinear behaviour of wood

Wood is an anisotropic material with different types of failure modes for shear, tension and compression stresses depending on the loading direction relative to its grain alignment. This means that the mechanical properties of wood (e.g. elastic moduli, shear moduli, Poisson's ratio and strength) vary with the directions and sign (i.e. whether in tension or compression). Based on previous experimental studies, the three most important failure modes can be identified and classified as [7]:

- Ductile failure due to compression parallel to the grain.
- Ductile failure due to compression perpendicular to the grain.
- Brittle failure due to shear parallel to the grain and tension perpendicular to the grain.

Fig. 1 shows the compression stress-strain curves of Scandinavian spruce with a mean density of  $430 \text{ kg/m}^3$  obtained experimentally by Karagiannis et al. [11]. It can be appreciated from this figure that, for the direction parallel to the grain (Fig. 1a), the behaviour is approximately linear elastic until the compressive strength is reached at around 40 MPa. After this point, a minor stress drop is produced followed by a plastic plateau. On the other hand, the compressive stress-strain relationship in the direction perpendicular to the grain (Fig. 1b) shows plastic behaviour with slight hardening after a strength of around 2.5 MPa is reached. It is important to note that the compressive strength in the direction perpendicular to the grain is less than 10% of the strength in the direction parallel to the grain.

The tension stress-strain curves of the same Scandinavian spruce material batch are shown in Fig 2. An initial linear elastic response followed by brittle failure is observed in both directions (parallel in Fig. 2a. and perpendicular to the grain in Fig. 2b). By contrast, the post-elastic behaviour in tension is markedly different due to absence of plastic deformation and the sudden loss of strength at failure. Besides, the tensile strength parallel to the grain (around 30 MPa) is also considerably higher than the tensile strength perpendicular to the grain (around 0.5 MPa).

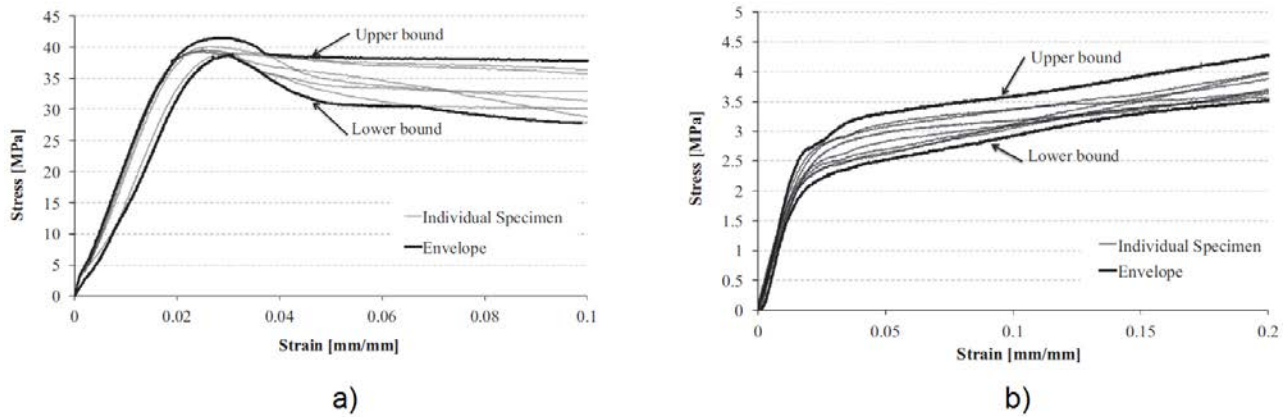


Fig. 1 – Scandinavian spruce compression stress-strain curve: a) Parallel to grain; b) Perpendicular to grain [11]

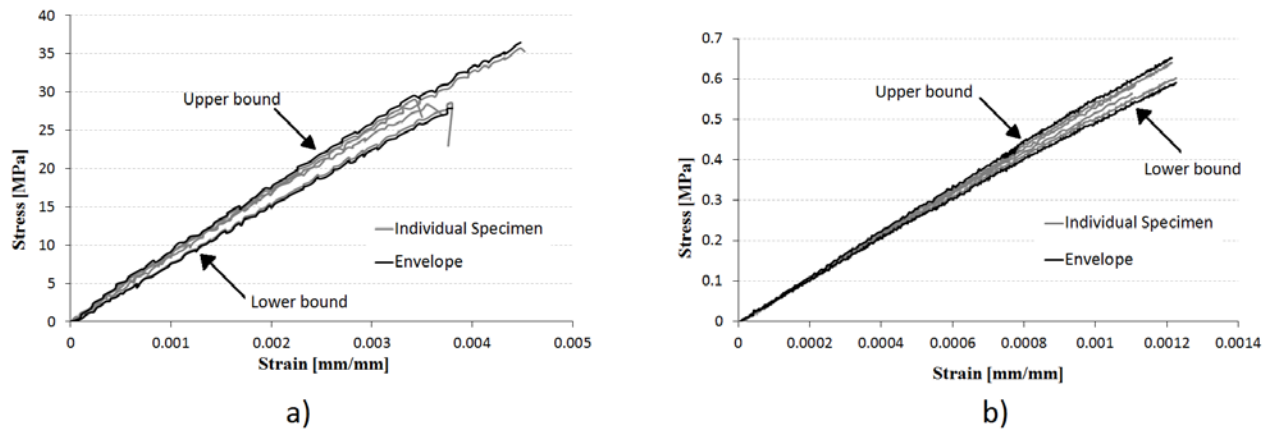


Fig. 2 – Scandinavian spruce tension stress-strain curve: a) Parallel to grain; b) Perpendicular to grain [12]

In light of the above discussion, timber failure modes can be summarized as ductile elastic-plastic failure with large deformation capacity for compressive stresses, and elastic brittle failure for the interaction of shear and tensile stresses. Based on this conclusion, a physically consistent constitutive model is proposed to study the nonlinear response of 3D timber structures subject to cyclic earthquake loading.

### 3. Orthotropic linear-elastic behaviour of timber

Before yielding (compression) or failure (tension and shear) is produced, the strain-stress constitutive equation is defined as:

$$\boldsymbol{\varepsilon} = \mathbf{C}^e : \boldsymbol{\sigma} \quad (1)$$

where  $\mathbf{C}^e$  is the fourth-order orthotropic linear-elastic compliance tensor, defined as a  $6 \times 6$  matrix in Voigt's notation such that:

$$\mathbf{C}^e = \begin{bmatrix} \frac{1}{E_X} & -\frac{\nu_{YX}}{E_Y} & -\frac{\nu_{ZX}}{E_Z} & 0 & 0 & 0 \\ -\frac{\nu_{XY}}{E_X} & \frac{1}{E_Y} & -\frac{\nu_{ZY}}{E_Z} & 0 & 0 & 0 \\ -\frac{\nu_{XZ}}{E_X} & -\frac{\nu_{YZ}}{E_Y} & \frac{1}{E_Z} & 0 & 0 & 0 \\ 0 & 0 & 0 & \frac{1}{G_{XY}} & 0 & 0 \\ 0 & 0 & 0 & 0 & \frac{1}{G_{YZ}} & 0 \\ 0 & 0 & 0 & 0 & 0 & \frac{1}{G_{ZX}} \end{bmatrix} \quad (2)$$

The orthotropic directions X, Y and Z correspond to the longitudinal, transverse and radial timber local axes, respectively. It is assumed that the longitudinal axis direction is parallel to the grain of the timber material, while the transverse and radial axes lay in the cross-section plan and act in the direction perpendicular to the grain. Notice that due to timber anisotropy the values of the elastic moduli, the shear moduli and the Poisson's ratios are different for each of the three orthogonal axes or planes. However, due to the symmetry property of  $\mathbf{C}^e$  and  $\mathbf{D}^e$ , the following conditions hold for the Poisson's ratios and the elastic moduli:

$$\frac{\nu_{XY}}{E_X} = \frac{\nu_{YX}}{E_Y}; \quad \frac{\nu_{YZ}}{E_Y} = \frac{\nu_{ZY}}{E_Z}; \quad \frac{\nu_{XZ}}{E_X} = \frac{\nu_{ZX}}{E_Z} \quad (3)$$

As a consequence, in order to define the linear-elastic orthotropic behaviour of timber, a total of nine mechanical material parameters are required: three elastic moduli, three shear moduli and three Poisson's ratios. Nevertheless, transverse isotropy is generally assumed for timber, reducing the number of independent parameters to five ( $E_X, E_Z, G_{ZX}, \nu_{XZ}, \nu_{ZY}$ ), by means of the following additional set of relations:

$$E_Y = E_Z; \quad G_{XY} = G_{ZX}; \quad \nu_{XZ} = \nu_{XY}; \quad G_{YZ} = \frac{E_Z}{2(1+\nu_{ZY})} \quad (4)$$

#### 4. Strain-based isotropic damage model for timber

Brittle failure due to tension and shear stresses generates voids and micro cracks in the timber matrix which not only lead to a sudden reduction of the material strength, but also cause a gradual degradation of its mechanical properties, including its stiffness. When further loading is applied, the micro-cracks grow and their coalescence produce macro-cracks zones and irreversible damage [8]. Continuum damage mechanics (CDM), based on the Thermodynamics of Irreversible Processes theory, has been widely used for modelling the nonlinear behaviour of different brittle materials, like concrete, rock [13], and more recently, timber [6]. Within CDM theory, strain-based damage models rely on the concept of Effective Stress and the hypothesis of Strain Equivalence. The former is defined as the stress acting in the reduced undamaged net surface area of the material, without considering the portion of area taken by the micro-cracks and voids. Taking into account that the total force acting in the material body is constant, the magnitude of the effective stress acting in the reduced undamaged area is higher than the magnitude of the Cauchy stress acting over the total nominal surface area. On the other hand, the hypothesis of strain equivalence states that the strain associated with the Cauchy stress in the damaged state is equivalent to the strain associated with the effective stress in the undamaged state [13].

The effective stress tensor  $\bar{\boldsymbol{\sigma}}$  is transformed into the Cauchy stress tensor  $\boldsymbol{\sigma}$  by means of the fourth-order tensor  $\mathbf{M}$ , which is a function of the fourth order damage tensor  $\mathbf{D}$  [14]:

$$\boldsymbol{\sigma} = \mathbf{M}(\mathbf{D}) : \bar{\boldsymbol{\sigma}} \quad (5)$$

Anisotropic damage is considered by assigning different values to the damage variables components of tensor  $\mathbf{D}$ . However, in spite of being an anisotropic material, there are two main disadvantages of including anisotropic damage in the timber material model, one physical and the other numerical. First, the evolution laws for the damage variables of the stress terms in each orthotropic direction are not known and difficult to obtain through experimental tests. Second, the strain equivalence hypothesis is not valid for anisotropic damage, and therefore, it is not possible to obtain a mechanically consistent anisotropic damage tensor without losing the symmetry of the Cauchy or the effective stress tensors. Given that, by definition, the Cauchy stress tensor is symmetric, a non-

symmetric effective stress tensor would need to be utilised [15]. The reasons for keeping the effective stress tensor symmetric will be explained below.

In light of the discussion above, isotropic damage is considered herein as the best option for the development of a mechanically consistent damage model. One of the most common and successful techniques for modelling isotropic damage consists of replacing both tensors  $\mathbf{M}$  and  $\mathbf{D}$  in Eq.(5) by a scalar expression, which for the particular case of isotropic damage takes the form:

$$\boldsymbol{\sigma} = (1 - \omega)\bar{\boldsymbol{\sigma}} \quad (6)$$

where  $\omega$  is the scalar damage variable. The damage process starts with the fulfilment of the damage criteria condition. Once this damage criteria is met, the value of the damage variable increases gradually and monotonically from 0 (undamaged state) to 1 (total damage state).

On the other hand, a timber material constitutive model for cyclic loading should be capable of reproducing the different inelastic responses of wood in tension and compression. This does not only include the different strengths and failure modes, but also the different post-elastic strength and stiffness degradation. The latter is particularly important in order to capture correctly the unloading-stiffness degradation and the stiffness recovery after load reversal, when passing from tension to compression stress states and vice versa [16]. For this reason, a split of the effective stress tensor into a tensile ( $\bar{\boldsymbol{\sigma}}^+$ ) and a compressive ( $\bar{\boldsymbol{\sigma}}^-$ ) components is performed such that:

$$\bar{\boldsymbol{\sigma}}^+ = \sum_{i=1}^3 \langle \bar{\sigma}_i \rangle \mathbf{p}_i \otimes \mathbf{p}_i \quad (7)$$

$$\bar{\boldsymbol{\sigma}}^- = \bar{\boldsymbol{\sigma}} - \bar{\boldsymbol{\sigma}}^+ \quad (8)$$

where  $\mathbf{p}_i$  and  $\bar{\sigma}_i$  are the eigenvectors and eigenvalues of the effective stress tensor, respectively. In this way, it becomes possible to manage independent damage mechanisms for tension and compression [1]. In order to obtain the principal values ( $\bar{\sigma}_i$ ) of the effective stress tensor and their associated unit eigenvectors ( $\mathbf{p}_i$ ), a spectral decomposition is performed. This justifies the selection of a symmetric effective stress tensor, and thus, of an isotropic damage model. The Macaulay brackets operator  $\langle \cdot \rangle$  in Eq (7) returns the positive values and sets the negative ones to zero. Thus, only the positive (tensile) principal stresses are retained. Finally, the scalar isotropic damage relationship between the Cauchy and the effective stress tensors in Eq. (6) can be reformulated in terms of the tensile and compressive components as:

$$\boldsymbol{\sigma} = (1 - \omega^+) \bar{\boldsymbol{\sigma}}^+ + (1 - \omega^-) \bar{\boldsymbol{\sigma}}^- \quad (9)$$

The initiation of the damage evolution process (when the damage variable  $\omega^\pm$  starts its gradual growth from 0 to 1) is determined by the damage criterion function defined as:

$$f_d^\pm(\bar{\boldsymbol{\sigma}}^\pm, r^\pm) = \bar{\tau}^\pm - r^\pm \quad (10)$$

This function is expressed in terms of an effective stress-based norm, called “equivalent stress” ( $\bar{\tau}^\pm$ ), and a threshold variable ( $r^\pm$ ) which controls the size of the damage surface. Notice that Eq. (10) encompasses two damage functions with different equivalent stresses and threshold variables for each independent tension and compression damage processes. Due to the anisotropy, complex stress interaction and failure characteristics of wood, a multidimensional damage function based on Hill’s criterion is adopted herein. Hence, the associated equivalent stress of the Hill’s damage criterion is defined in Voigt’s notation as:

$$\bar{\tau}^\pm = \sqrt{\frac{3}{2} \bar{\boldsymbol{\sigma}}^{\pm T} \mathbf{P}^\pm \bar{\boldsymbol{\sigma}}^\pm} \quad (11)$$

where the equivalent stress,  $\bar{\tau}^\pm$ , is defined for both, tension and compression failure, in terms of the corresponding effective stress tensor  $\bar{\boldsymbol{\sigma}}^\pm$  and the strength parameters matrices  $\mathbf{P}^\pm$ .

On the other hand, the variation of the damage variable  $\omega^\pm$  in function of the threshold variable  $r^\pm$  is governed by the damage evolution law:

$$\omega^\pm = g_d^\pm(r^\pm) \quad (12)$$

The mathematical expression of this monotonically increasing function is related to the post-elastic stress behaviour (e.g. softening, perfect plasticity, hardening) by means of Eq. (6). This relationship is more clearly expressed in terms of the initial threshold variable  $r_0^\pm$  and the uniaxial normal strength  $f_{max}$  as:

$$\sigma = \frac{r^\pm}{r_0^\pm} f_{max} (1 - g_d^\pm(r^\pm)) \quad (13)$$

Four damage evolution laws employed elsewhere to model tensile softening behaviour [1, 4, 6, 17] are reproduced in Figs. 3a and 3b for the Cauchy stress  $\sigma$  and the associated damage variable  $\omega$ , respectively.

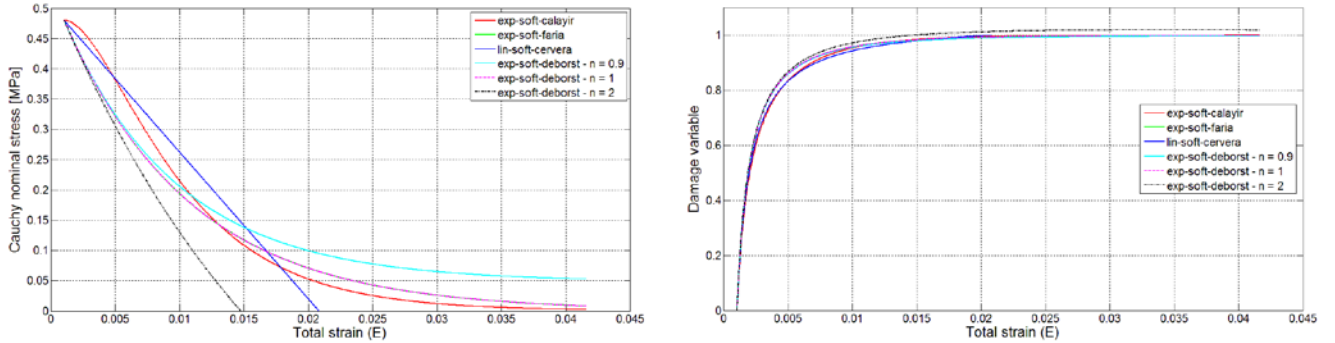


Fig. 3 – Damage evolution law for tensile softening [1, 4, 6, 17]: a) Cauchy stress; b) Damage variable

De Borst et al. [4] proposed a versatile damage evolution law for modelling different exponential softening responses:

$$g_d^+(r^+) = 1 - \frac{r_0^+}{r^+} (1 - n + n \times e^{-b(r^+ - r_0^+)}) \quad (14)$$

where

$$b = \frac{A}{n \times r_0^+}; \quad A = \frac{2H}{1-H}; \quad H = \frac{(f_Z^+)^2 \times l_{ch}}{2 \times G_{f,Z} \times E_Z} \quad (15)$$

and  $n$  is a calibration parameter. For  $n$  smaller than 1, asymptotically exponential softening is observed in Fig. 3a. The lower the value of  $n$ , the higher the residual strength obtained even for widespread damage levels. On the contrary, for values of  $n$  higher than 1, there is no asymptotic behaviour and the stress rapidly decays to zero. For this reason, and based on the behaviour observed in Fig. 2, Eqs. (14) and (15) were selected to represent the timber damage evolution for tensile softening. In the case of compressive post-elastic behaviour, the definition of the damage evolution law is straightforward. Fig. 1 shows that perfect plasticity can accurately represent the timber ductile failure in compression. Therefore,  $g_d^-(r^-)$  can be defined as [6]:

$$g_d^-(r^-) = 1 - \frac{r_0^-}{r^-} \quad (16)$$

Finally, the damage model is completely defined by the damage function, Eq. (10), the damage evolution law, Eq. (12), and loading-unloading (Kuhn-Tucker) conditions defined as:

$$f_d^\pm \leq 0; \quad \dot{r}^\pm \geq 0; \quad \dot{r}^\pm f_d^\pm = 0 \quad (17)$$

where

$$r^\pm = \max\{r_0^\pm, \max_{0 \leq x \leq t}(\bar{\tau}_x^\pm)\} \quad (18)$$

## 5. Plasticity with isotropic hardening model for timber

The damage model described in the previous section entails the definition of two parallel stress spaces (nominal and effective). Two alternative approaches for coupling the plasticity and damage parts of the model are possible

depending on in which space the plasticity part of the model is formulated (i.e. whether plasticity is formulated in the nominal Cauchy stress space or in the effective stress space). From a physical point of view, plasticity in compression occurs in the material matrix, between voids and cracks, leading to local hardening behaviour [18]. This means that the effective stress tensor, which is defined to act only over the undamaged material matrix, offers a more consistent stress space for the plasticity formulation [13]. Furthermore, it is important to consider potential numerical issues when defining the plasticity stress space. In order to obtain a unique solution (Local Uniqueness Condition), plasticity algorithms based on nominal stresses require the introduction of strong hardening [3]. However, Fig. 1 shows that perfect plasticity (parallel to the grain) and slight hardening plasticity (perpendicular to the grain) are characteristic of timber nonlinear behaviour under compressive stresses. Therefore, a nominal stress based plasticity model, which requires the introduction of strong hardening in order to be numerically stable, is not a suitable alternative for wood. By contrast, in the effective stress space, hardening plasticity is not a requirement of the local uniqueness [3]. In light of this, this study employs an effective-space stress formulation. This is another important reason for ensuring the symmetry of the effective stress tensor, by coupling the plasticity model with a scalar isotropic damage model, as mentioned above.

Based on the characteristic strain tensor decomposition of plasticity theory, the relationship between the effective stress  $\bar{\sigma}$ , the total strain  $\boldsymbol{\varepsilon}$ , the elastic strain  $\boldsymbol{\varepsilon}^e$  and the plastic strain  $\boldsymbol{\varepsilon}^p$  is defined as:

$$\bar{\sigma} = \mathbf{D}^e : \boldsymbol{\varepsilon}^e = \mathbf{D}^e : (\boldsymbol{\varepsilon} - \boldsymbol{\varepsilon}^p) \quad (19)$$

The three components of the plasticity model are the yield function, the plasticity flow rule and the hardening variable evolution law. As before, the Hill criterion equivalent stress defined in Eq. (11) is employed herein for the definition of the plasticity orthotropic yield function [19]:

$$f_p = \sqrt{\frac{3}{2} \bar{\boldsymbol{\sigma}}^{-T} \mathbf{P}^- \bar{\boldsymbol{\sigma}}^-} - \bar{\sigma}_y(k^p) \quad (20)$$

where the reference yield stress,  $\bar{\sigma}_y$ , is a function of the plastic hardening variable  $k^p$ . Notice that, in agreement with the observed experimental behaviour and the timber material modelling hypothesis, the yield function is defined only for the compressive part of the effective stress tensor,  $\bar{\boldsymbol{\sigma}}^-$ . Accordingly, the Hill criterion employed in the yield function is formulated only in terms of the compression strength parameters matrix  $\mathbf{P}^-$ . Thus, the proposed model considers a damage-only behaviour in tension with no plastic response.

The flow rule expression for associated plasticity is given by:

$$\dot{\boldsymbol{\varepsilon}}^p = \dot{\lambda} \mathbf{n}(\bar{\boldsymbol{\sigma}}^-, k^p); \quad \mathbf{n} = \frac{\partial f_p(\bar{\boldsymbol{\sigma}}^-, k^p)}{\partial \bar{\boldsymbol{\sigma}}^-} \quad (21)$$

Eq. (21) is expressed in terms of the plastic multiplier  $\dot{\lambda}$  and the first order differentiation tensor  $\mathbf{n}$  of the yield function with respect to the compressive effective stress. Likewise, the normalized work-hardening hypothesis evolution law is defined as:

$$\dot{k}^p = \dot{\lambda} p(\bar{\boldsymbol{\sigma}}^-, k^p); \quad p = \frac{1}{\bar{\sigma}_y(k^p)} \bar{\boldsymbol{\sigma}}^- : \mathbf{n}(\bar{\boldsymbol{\sigma}}^-, k^p) \quad (22)$$

where  $p$  is a scalar function of the compressive effective stress tensor and the plastic hardening variable. Finally, the following loading-unloading conditions complete the formulation of the plasticity model:

$$f_p \leq 0; \quad \dot{\lambda} \geq 0; \quad \dot{\lambda} f_p = 0 \quad (23)$$

For the particular Hill yield function defined in Eq. (20), the expression of the plastic flow direction vector  $\mathbf{n}$ , normal to the yield surface and defined in Eq. (21), can be determined in Voigt's notation as:

$$\mathbf{n} = \frac{3}{2\bar{\sigma}_y(k^p)} \mathbf{P}^- \bar{\boldsymbol{\sigma}}^- \quad (24)$$

In Eq. (24) the plastic flow condition  $f_p = 0$  was used to express the plastic flow direction vector in terms of the reference yield stress  $\bar{\sigma}_y$ . Using the same condition after replacing Eq. (24) into Eq. (22) leads to the conclusion that, for Hill's associated plasticity in combination with this particular work-hardening evolution law, the value of the function  $p$  is constant and equal to 1 ( $p = 1$ ). Therefore, the hardening law of Eq. (22) can be reduced to:

$$\dot{k}^p = \dot{\lambda} \quad (25)$$

while the hardening modulus can be expressed only in terms of the reference yield stress,  $\bar{\sigma}_y$ , and the hardening variable,  $k^p$  as:

$$h = -\frac{\partial f_p(\bar{\sigma}^-, k^p)}{\partial k^p} = \frac{d\bar{\sigma}_y(k^p)}{dk^p} \quad (26)$$

Similarly, the hardening modulus can be expressed in terms of the compressive strength and the derivative of the uniaxial effective stress with respect to the plastic strain in the Z direction (perpendicular to the grain):

$$h = \frac{1}{(f_z^-)^2} \frac{\partial \bar{\sigma}_z^-}{\partial \varepsilon_z^p} \quad (27)$$

The following expression can be used to calculate the derivative of the uniaxial effective stress with respect to the plastic strain in terms of the elastic  $E_Z$  and tangent  $T_Z$  moduli:

$$\frac{\partial \bar{\sigma}_z^-}{\partial \varepsilon_z^p} = \frac{E_Z \cdot T_Z}{E_Z - T_Z} \quad (28)$$

The terms of Eq. (28) are represented in Fig. 4, which shows the bi-linear uniaxial stress-total strain diagram in the Z axis. For timber in compression perpendicular to the grain, it can be assumed that  $T_Z = 0.1 \times E_Z$  [10]. Thus, the hardening modulus is an input parameter of the plasticity model which can be calculated from the bi-linear uniaxial stress-total strain diagram and the compressive strength in the direction perpendicular to the grain.

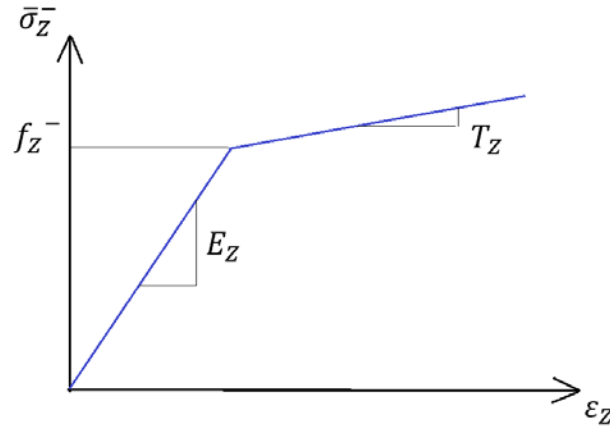


Fig. 4 – Bi-linear uniaxial stress-total strain in the Z axis (direction perpendicular to the grain)

The backward Euler method (fully implicit) is employed to integrate the stress-strain rate equations. To this end, the finite increment counterpart of the plasticity flow rule in Eq. (21) is expressed as:

$$\Delta \varepsilon^p = \Delta \lambda \mathbf{n}(\bar{\sigma}^-, k^p) \quad (29)$$

Correspondingly, Eq. (19) is also reformulated in terms of finite increments in compression:

$$\Delta \bar{\sigma}^- = \mathbf{D}^e \Delta \varepsilon^- - \Delta \lambda \mathbf{D}^e \mathbf{n}(\bar{\sigma}^-, k^p) \quad (30)$$

Besides, at the beginning of the load increment, the total strain increment  $\Delta \varepsilon^-$ , the initial effective stress  $\bar{\sigma}_j^-$  and the hardening modulus  $h$  are known. The addition of  $\bar{\sigma}_j^-$  to both sides of Eq. (30) makes it possible to obtain the final effective stress  $\bar{\sigma}_{j+1}^-$  as an elastic predictor-plastic corrector process:

$$\bar{\sigma}_{j+1}^- = \bar{\sigma}^e - \Delta \lambda \mathbf{D}^e \mathbf{n}(\bar{\sigma}_{j+1}^-, k_{j+1}^p); \quad \bar{\sigma}^e = \bar{\sigma}_j^- + \mathbf{D}^e \Delta \varepsilon^- \quad (31)$$

It should be noted that, hereafter, all the equations are formulated in Voigt's notation. Two additional finite increment equations can be derived from the hardening law in Eq. (25) and the yield function in Eq. (20), respectively, such that :

$$k_{j+1}^p = k_j^p + \Delta\lambda \quad (32)$$

$$f_p = \sqrt{\frac{3}{2} \bar{\sigma}_{j+1}^T \mathbf{P}^- \bar{\sigma}_{j+1}} - \bar{\sigma}_y(k_{j+1}^p) = 0 \quad (33)$$

In this way, the systems of three nonlinear equations (Eqs. (31) to (33)) with three unknowns ( $\bar{\sigma}_{j+1}$ ,  $k_{j+1}^p$  and  $\Delta\lambda$ ) is completely defined. These three equations can be combined and reduced to only one equation with one unknown. By substituting Eq. (24) into Eq. (31) and after rearranging the final effective stress the following expressions are obtained:

$$\bar{\sigma}_{j+1} = \mathbf{A}^{-1}(\Delta\lambda) \bar{\sigma}_e; \quad \mathbf{A} = \mathbf{I} + \frac{3 \cdot \Delta\lambda}{2 \cdot \bar{\sigma}_y(\Delta\lambda)} \mathbf{D}^e \mathbf{P}^- \quad (34)$$

Finally, after replacing Eq. (34) into Eq. (33) a single nonlinear scalar equation with one unknown (the plastic multiplier increment) is obtained:

$$\sqrt{\frac{3}{2} \bar{\sigma}_e^T (\mathbf{A}^{-1})^T \mathbf{P}^- \mathbf{A}^{-1} \bar{\sigma}_e} - \bar{\sigma}_y(\Delta\lambda) = 0 \quad (35)$$

Therefore, the plasticity problem is reduced to the solution of Eq. (35) by means of an iterative method like Newton-Raphson. Once the plastic multiplier increment  $\Delta\lambda$  is determined, the effective stress  $\bar{\sigma}_{j+1}$ , the hardening variable  $k_{j+1}^p$  and the plastic strain vector increment  $\Delta\boldsymbol{\epsilon}^p$  are explicitly obtained by means of Eqs. (34), (32) and (29), respectively.

## 6. Test examples: Uniaxial stress-strain cyclic response

The plasticity-damage model proposed here was implemented and the stress-strain response of a timber specimen subjected to uniaxial cyclic loading in parallel and perpendicular to the grain directions were numerically obtained. To this end, the material model parameters presented in Table 1 were employed. As discussed in Section 3, these material properties correspond to the assumption of timber orthotropic behaviour with transverse isotropy.

Figs. 5 and 6 show the cyclic stress-strain response of the timber material model when subjected to uniaxial loading in the direction parallel (X) and perpendicular (Y) to the grain, respectively. In both cases it can be observed that the responses under tensile and compressive stress states are completely different. The tensile inelastic response is characterised by exponential softening, while the compressive counter-part by plasticity with hardening. Accordingly, permanent plastic deformations occur in the negative side of the strain axis when the stress passes from compression to tension. Moreover, the level of stiffness degradation in tension is significantly higher than in compression. This is due to the lower strength and the damage-only (no plasticity) response of tensile stresses, which derive in a secant unloading stiffness. On the other hand, the higher strength in compression and the inclusion of plasticity generate a milder stiffness degradation with an unloading stiffness in-between the elastic and the secant. Consequently, Figs. 5 and 6 show the model capability to reproduce stiffness recovery after tension-compression loading reversal, and vice versa.

Table 1 – Timber material model parameters

|   |                                  |                                 |                                  |
|---|----------------------------------|---------------------------------|----------------------------------|
| <b>Poisson's ratio</b>                          | $\nu_{XY} = 5.95 \times 10^{-1}$ | $\nu_{YZ} = 4.1 \times 10^{-1}$ | $\nu_{ZX} = 5.95 \times 10^{-1}$ |
| <b>Shear moduli [kN/mm<sup>2</sup>]</b>         | $G_{XY} = 8.5 \times 10^{-1}$    | $G_{YZ} = 1.63 \times 10^{-1}$  | $G_{ZX} = 8.5 \times 10^{-1}$    |
| <b>Young moduli [kN/mm<sup>2</sup>]</b>         | $E_X = 1.16 \times 10^1$         | $E_Y = 4.6 \times 10^{-1}$      | $E_Z = 4.6 \times 10^{-1}$       |
| <b>Compressive strength [kN/mm<sup>2</sup>]</b> | $f_X^- = 3.9 \times 10^{-2}$     | $f_Y^- = 3.3 \times 10^{-3}$    | $f_Z^- = 3.3 \times 10^{-3}$     |
| <b>Tensile strength [kN/mm<sup>2</sup>]</b>     | $f_X^+ = 1.98 \times 10^{-2}$    | $f_Y^+ = 4.8 \times 10^{-4}$    | $f_Z^+ = 4.8 \times 10^{-4}$     |

|  |                                |                               |                               |
|--|--------------------------------|-------------------------------|-------------------------------|
| <b>Shear strength [kN/mm<sup>2</sup>]</b>    | $f_{XY} = 3.8 \times 10^{-3}$  | $f_{YZ} = 3.8 \times 10^{-3}$ | $f_{ZX} = 3.8 \times 10^{-3}$ |
| <b>Fracture energy density [kN/mm]</b>       | $G_{f,Z} = 5.0 \times 10^{-4}$ |                               |                               |
| <b>Exponential softening parameter</b>       | $n = 1.0$                      |                               |                               |
| <b>Hardening modulus [mm<sup>2</sup>/kN]</b> | $h = 4.7 \times 10^3$          |                               |                               |

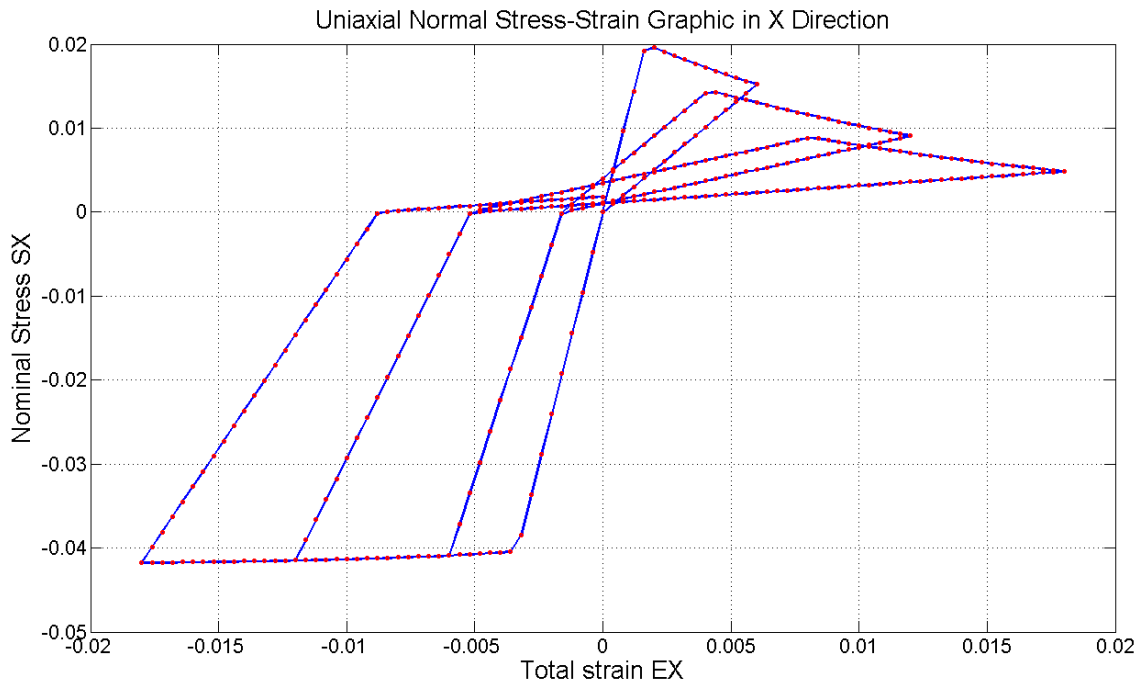


Fig. 5 – Plasticity-damage model: uniaxial cyclic loading-unloading stress-strain diagram in the direction parallel to the grain

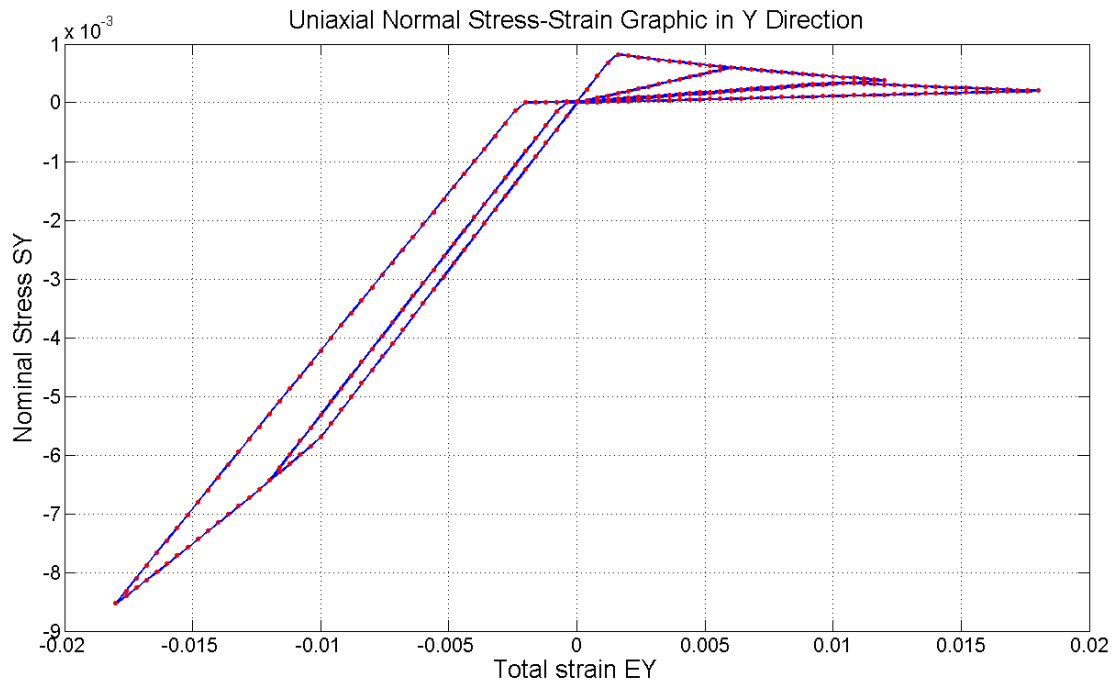


Fig. 6 – Plasticity-damage model: uniaxial cyclic loading-unloading stress-strain diagram in the direction perpendicular to the grain

Finally, it is worthy noting that for the cyclic uniaxial loading perpendicular to the grain (Fig. 6), the compressive nominal stress corresponding to the beginning of the inelastic plasticity-damage response is considerably higher than the compressive strength in Y-direction shown in Table 1. The reason for this is the presence of confining compressive stresses along the orthogonal directions X and Z. Under this triaxial compressive stress state, the multidimensional Hill yield criterion requires the interaction of higher stresses in the three directions before the yielding state is initiated. Due to its comparatively higher resistance, this phenomena has a minor influence in the parallel-to-the-grain compressive non-linear response. Overall, the proposed model captures the key characteristics of the cyclic behaviour of timber materials but, due to the absence of directly comparable tests at the local material level, future validation will need to be carried against component tests following implementation in a finite element program.

## 7. Conclusions

This article presented the development of a theoretical framework and the formulation required for the implementation of a 3D plasticity-damage constitutive model for timber materials. The suitability of such a model to reproduce cyclic non-linear response of timber was of particular importance. In light of the preliminary numerical results obtained for uniaxial loading, it was concluded that the coupling of orthotropic plasticity in compression with isotropic damage in both tension and compression stress states, provides a very promising approach for the modelling of timber structures subjected to earthquake loading. Tensile softening brittle failure, stiffness cyclic degradation and recovery after load-reversal, in addition to compressive permanent plastic deformation, are some of the most important characteristics of timber non-linear behaviour which can be captured by the proposed constitutive model. Further research work is currently being developed to implement the model algorithm in the framework of a commercial FE software user-supplied subroutine, with the objective of calibrating and validating it against experimental results on timber components and structures.

## 8. Acknowledgements

The authors wish to acknowledge the support of the Department of Civil and Environmental Engineering of Imperial College London and Perú Government CONCYTEC/CIENCIACTIVA Program.

## 9. References

- [1] Faria R, Oliver J, Cervera M (1998): A strain-based plastic viscous-damage model for massive concrete structures. *International Journal of Solids and Structures*, 35(14), 1533–1558.
- [2] Lee J, Fenves GL (1998): Plastic-Damage Model for Cyclic Loading of Concrete Structures. *Journal of Engineering Mechanics ASCE*, 124(8), 892–900.
- [3] Grassl P, Jirasek M (2006): Damage-plastic model for concrete failure. *International Journal of Solids and Structures*, 43(22-23), 7166–7196.
- [4] De Borst R, Pamin J, Geers MGD (1999): On coupled gradient-dependent plasticity and damage theories with a view to localization analysis. *European Journal of Mechanics, A/Solids*, 18(6), 939–962.
- [5] Franke B, Quenneville P (2011): Numerical Modeling of the Failure Behavior of Dowel Connections in Wood. *Journal of Engineering Mechanics*, 137(3), 186–195.
- [6] Sandhaas C, Van de Kuilen JW, Blass HJ (2012): Constitutive Model for Wood Based on Continuum Damage Mechanics. *World Conference on Timber Engineering*, Auckland, New Zealand.
- [7] Xu B, Bouchair A, Racher P (2014): Appropriate Wood Constitutive Law for Simulation of Nonlinear Behavior of Timber Joints. *J. Mater. Civ. Eng. (ASCE)*, 26, 1–7.
- [8] Khelifa M, Khennane A, El Ganaoui M, Celzard A (2015): Numerical damage prediction in dowel connections of wooden structures. *Materials and Structures*. doi:10.1617/s11527-015-0615-5
- [9] Kharouf N, McClure G, Smith I (2005): Postelastic Behavior of Single- and Double-Bolt Timber Connections. *Journal of Structural Engineering*, 131(1), 188–196.
- [10] Xu BH, Bouchair A, Taazount M, Racher P (2013): Numerical simulation of embedding strength of glued laminated timber for dowel-type fasteners. *Journal of Wood Science*, 59(1), 17–23.
- [11] Karagiannis V (2016): Structural response of hybrid steel-timber joints. PhD Thesis, Imperial College London, Department of Civil and Environmental Engineering, London, UK (in preparation).
- [12] Karagiannis V, Málaga-Chuquitaype C, Elghazouli AY (2016): Modified foundation modelling of dowel embedment in glulam connections. *Construction and Building Materials*, 102(2), 1168–1179.
- [13] Simo JC, Ju JW (1987): Strain- and stress-based continuum damage models—I. Formulation. *International Journal of Solids and Structures*, 23(7), 821–840.
- [14] Ju JW (1991): Isotropic and Anisotropic Damage Variables in Continuum Damage Mechanics. *Journal of Engineering Mechanics ASCE*, 116(12), 2764–2770.
- [15] Valliappan S, Yazdchi M, Khalili N (1999): Seismic analysis of arch dams—a continuum damage mechanics approach. *International Journal for Numerical Methods in Engineering*, 45(11), 1695–1724.
- [16] Matzenmiller A, Lubliner J, Taylor RL (1995): A constitutive model for anisotropic damage in fiber-composites. *Mechanics of Materials*, 20(2), 125–152.
- [17] Calayir Y, Karaton M (2005): A continuum damage concrete model for earthquake analysis of concrete gravity dam-reservoir systems. *Soil Dynamics and Earthquake Engineering*, 25(11), 857–869.
- [18] De Borst, R (2001): Some recent issues in computational failure mechanics. *International Journal for Numerical Methods in Engineering*, 52(12), 63–95.
- [19] De Borst R, Feenstra PH (1990): Studies in Anisotropic Plasticity with Reference to the Hill Criterion. *International Journal of Numerical Methods in Engineering*, 29, 315–336.